Available online at www.sciencedirect.com
SCIENCE DIRECT®
Journal of Organometallic Chemistry 688 (2003) 236–245
Journal of Organometallic Chemistry
www.elsevier.com/locate/jorganchem

Electrochemical behavior of the Cp*(dithiolato)Co(III) complex [(η^5-Cp*)Co(1,2-$S_2C_2B_{10}H_{10}$-*S*,*S*′)] and its derivatives: the effect of the ligand on half-sandwich cobalt(III) complexes

Bo Young Kim [a], Chongmok Lee [a,*], Seung Won Chung [b], Young-Joo Lee [b], JaeYoun Pak [a], Jaejung Ko [b,*], Sang Ook Kang [b,*]

[a] *Department of Chemistry, Ewha Woman's University, Seoul 120-750, South Korea*
[b] *Department of Chemistry, Korea University, 208 Seochang, Chochiwon, Chung-nam 339-700, South Korea*

Received 5 July 2003; received in revised form 4 September 2003; accepted 11 September 2003

Abstract

Reaction of the 16-electron dithiolatocobalt, [(η^5-Cp*)Co($Cab^{S,S'}$)] (**1**) ($Cab^{S,S'}$ = 1,2-$S_2C_2B_{10}H_{10}$-*S*,*S*′), with a ligand L (L = CN^tBu, PMe_3, PEt_3, $PHPh_2$) affords the 18-electron complexes [(η^5-Cp*)Co($Cab^{S,S'}$)(L)] (**2**) in high yield. The structures of **2** in solution were probed by NMR spectroscopy, and the solid-state structure of the diphenylphosphine derivative was established by single-crystal X-ray diffraction. Cyclic voltammetry of **1** shows that the complex undergoes a quasi-reversible one-electron oxidation and reversible reduction. The voltammetry of the corresponding 18-electron complex **2** was investigated rather extensively in terms of coordination and redox chemistry, in which the influence of the enhanced steric interaction between the bulky Cp* and incoming ligand could be observed. Cyclic voltammograms of alkylidiene or acetylene adducts of dithiolatocobalt complex **1**, [(η^5-Cp*)Co{η^3-(*S*,*S*′,*C*′)-$SC_2B_{10}H_{10}S(C'R_2)$}] [$C'R_2$ = $CHSiMe_3$ (**3a**), HC=CPh (**3b**), (COOMe)C=C(COOMe) (**3c**)], are also included.
© 2003 Elsevier B.V. All rights reserved.

Keywords: Dithiolatocobalt; 18-Electron dithiolate; Redox process; Cyclic voltammetry

1. Introduction

We recently reported new coordination modes for coordinatively unsaturated half-sandwich metal complexes [1] possessing an ancillary dithio-*o*-carboranyl ligand [2], in which the redox stability of the complexes was dependent on the ancillary ligand Cp or Cp*. For example, (η^5-Cp)Co($Cab^{S,S'}$) (**I**) reacts with BH_3·THF to give a dinuclear complex of [(η^5-CpCo)$_2$($Cab^{S,S'}$)], while (η^5-Cp*)Co($Cab^{S,S'}$) (**1**) was suppressed from making the corresponding dinuclear complex probably due to the bulkiness of the Cp* ligand (Chart 1) [3].

The redox patterns of mononuclear and dinuclear complexes are different from each other. Thus, the electrochemistry of **1** and its derivatives may provide a clearer view of the redox chemistry, since the mononuclear complexes will be free from dinuclear complexes. In our previous work with (η^5-Cp)Co($Cab^{S,S'}$) (**I**) [3] and (η^6-arene)Ru($Cab^{S,S'}$) (**II**) [4], we also found that 16-electron complexes had a reversible 0/−1 reduction with a much less reversible 0/+1 oxidation; the reversibility of the latter process was improved upon the addition of a ligand (i.e. it occurs via an 18-electron complex). However, we had some difficulties in observing the reversibility of the 0/−1 reduction, depending on coordination in the Ru complexes due to solvent window, and the 0/+1 oxidation in the cobalt complexes due to a lack of electron-donating ability of the Cp ligand. This redox pattern of 16- versus 18-electron complexes could be exemplified more clearly by 1 rather

* Corresponding authors. Tel.: +82-41-860-1334; fax: +82-41-867-5396.
E-mail address: sangok@korea.ac.kr (S.O. Kang).

0022-328X/03/$ - see front matter © 2003 Elsevier B.V. All rights reserved.
doi:10.1016/j.jorganchem.2003.09.019

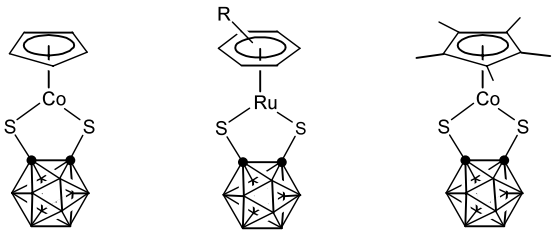

[(η^5-Cp)Co(Cab$^{S,S'}$)] **I** [(η^6-arene)Co(Cab$^{S,S'}$)] **II** [(η^5-Cp*)Co(Cab$^{S,S'}$)] **1**

Chart 1.

than I due to the stronger electron-donating ability of Cp*; therefore, this is one of the motivations for this study.

To explore the effects of ancillary Cp* ligand in terms of coordination and redox chemistry, we have synthesized a series of 18-electron dithiolates [(η^5-Cp*)Co(Cab$^{S,S'}$)(L)] (**2**) [L = CN^{t}Bu (**2a**), PMe_3 (**2b**), PEt_3 (**2c**), $PHPh_2$ (**2d**)] and [(η^5-Cp*)Co{η^3-(*S*,*S*′,C')-$SC_2B_{10}H_{10}S$(C'R_2)}] [C'R_2 = CHSiMe_3 (**3a**), HC=CPh (**3b**), (COOMe)C=C(COOMe) (**3c**)]. The comparison of these two dithiolatocobalts in terms of the ancillary ligands, Cp and Cp*, is our main interest because they possess the desired differences in electron-donating ability and structural bulkiness.

2. Results and discussion

2.1. Synthesis and spectroscopic characterization of [(η^5-Cp*)Co(Cab$^{S,S'}$)(L)] L = CN^{t}Bu (2a), PMe_3 (2b), PEt_3 (2c), $PHPh_2$ (2d))

Reaction of the 16-electron complex **1** with 2-electron donor molecules such as *tert*-butyl isocyanide and triethylphosphine gave various 18-electron complexes (Scheme 1). Our results are closely related to those of the reported 16-electron cobalt, ruthenium, rhodium, osmium, and iridium complexes such as (η^5-Cp)Co(Cab$^{S,S'}$) [3], (η^6-*p*-cymene)Ru(Cab$^{S,S'}$) [4], (η^5-Cp*)Rh(Cab$^{S,S'}$) [3], (η^6-*p*-cymene)Os(Cab$^{S,S'}$) [5], and (η^5-Cp*)Ir(Cab$^{S,S'}$) [1d].

Treatment of the mononuclear **1** with an excess of CN^{t}Bu in toluene gave the reddish-brown addition product [(η^5-Cp*)Co(Cab$^{S,S'}$)(CN^{t}Bu)] (**2a**) in 95% yield. The structure of **2a** was determined on the basis of IR and NMR spectra, as well as elemental analysis. Thus, complex **2a** exhibited a single CN stretching absorption at 2181 cm^{-1} in the IR spectrum, which is quite normal for a terminal Co–CNR ligand with significant π-back-bonding of the isocyanide ligand. The ^{1}H-NMR spectrum of **2a** had a singlet at δ 1.60 due to a *tert*-butyl moiety.

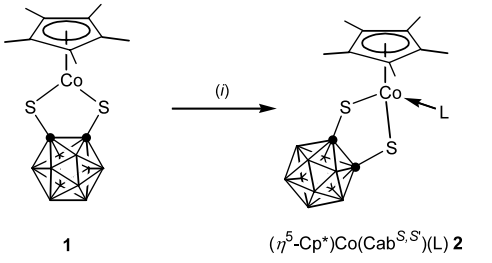

1 (η^5-Cp*)Co(Cab$^{S,S'}$)(L) **2**

Scheme 1. Addition reaction of 16-electron metal complexes **1** [a].

Reaction of **3** with an excess of PR_3 in toluene afforded red crystals of **2b**–**d** in 82–94% yield. The ^{31}P{^{1}H}-NMR of **2b**–**d** had a singlet at around δ 7.85–26.67. The ^{1}H-NMR data for **2b**–**d** were consistent with the structure of **2d** determined by an X-ray structural study. The ORTEP diagram in Fig. 1 shows the molecular structure of **2d** and confirms the six-coordinate geometry about the cobalt atom, assuming that the Cp* ring serves as a three-coordinate ligand. The Co atom environment is transformed from a two-legged piano-stool geometry in **1** to a three-legged version in **2** [6]. Overall, the structure is octahedral with an idealized C_s molecular symmetry, similar to that observed in other related complexes such as [(η^5-Cp)Co(Cab$^{S,S'}$)(PEt_3)] [3], [(η^5-Cp*)Ir(Cab$^{S,S'}$)(PMe_3)] [1d] and (η^6-*p*-cymene)Ru(Cab$^{S,S'}$)(L) (L = PPh_3, $P(OMe)_3$, NH_3, NC_5H_5, CO, CN^{t}Bu, SEt_2, SC_4H_8, CN^-, SCN^-) [5].

2.2. Electrochemistry of complexes 1 and 2

Electrochemical data obtained in CV experiments are summarized in Table 1. Fig. 2 shows cyclic voltammograms (CVs) of complexes **1** and **2a**–**d** in CH_2Cl_2 containing 0.1 M TBAB with a potential scan rate (v) of 0.1 V s^{-1}. The CV of **1** shows two major redox

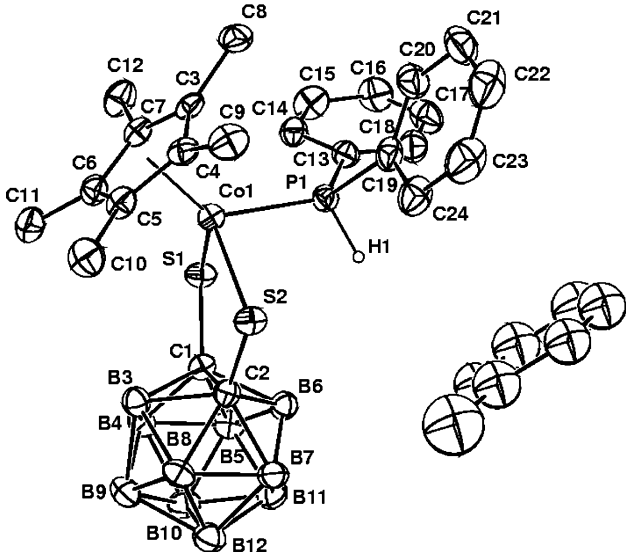

Fig. 1. Molecular structure of [(η^5-Cp*)Co(Cab$^{S,S'}$)($PHPh_2$)**2d**·C_7H_8) with atom labeling; ellipsoids show 30% probability levels and hydrogen atoms have been omitted for clarity.

Table 1
The peak potentials E_{pcn}(red) and E_{pan}(ox) of (η^5-Cp*)Co(Cab$^{S,S'}$)(L) from CV data

Compound	L	Reduction step		Oxidation step	
		E_{pc1} (V)	E_{pc2} (V)	E_{pa1} (V)	E_{pa2} (V)
1		−1.14		0.85	
2a	CN^{t}Bu	−1.66		0.60	
2b	PMe_3	−1.65		0.66	
2c	PEt_3	−1.14	−1.75	0.52	0.85
2d	$PHPh_2$	−1.04	−1.52	0.71	0.90
3a	η^1-CHSiMe$_3$–*S*	−1.10	−1.91	0.24	
3b	η^1-HC=CPh–*S*	−1.78		0.13	
3c	η^1-(COOMe)C=C(COOMe)–*S*	−1.37		0.59	

Potentials are recorded versus $E_{1/2}$ ($Fc^+|Fc$).

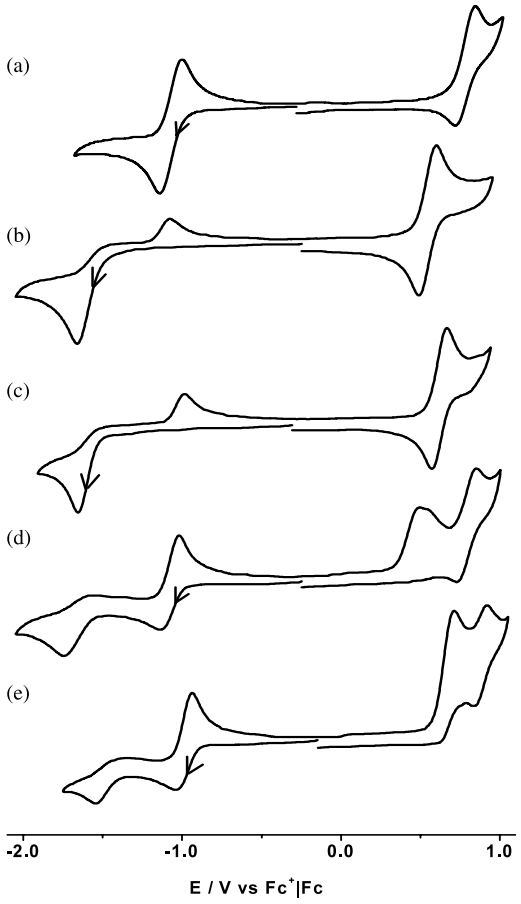

Fig. 2. Cyclic voltammograms (CVs) of (η^5-Cp*)Co(Cab$^{S,S'}$) (**1**) (A) and [(η^5-Cp*)Co(Cab$^{S,S'}$)(L)] [L = CN^{t}Bu (**2a**) (B), PMe_3 (**2b**) (C), PEt_3 (**2c**) (D), $PHPh_2$ (**2d**) (E)] at a platinum disk electrode with negative initial scan direction; in CH_2Cl_2 containing 0.1 M TBAB with the scan rate (v) of 0.1 V s^{-1}.

responses, that is, a reversible 0/−1 reduction wave of (Co^{3+}/Co^{2+}) at $E_{1/2} = -1.07$ V [3,6,7] and a quasi-reversible 0/+1 oxidation wave of the cobaltadithiolene ring at $E_{1/2} = 0.79$ V. The general pattern of the CV is the same as (η^5-Cp)Co(Cab$^{S,S'}$) (**I**) except for the corresponding potential values (for **I**, reduction occurs at $E_{1/2} = -0.59$ V and oxidation at $E_{pa} = 0.99$ V) and the improved reversibility of the oxidation wave. As the ligand was changed from Cp to Cp*, both the reduction and oxidation potentials shifted towards the negative direction by 0.48 and 0.14 V, respectively; this indicates the stronger electron-donating ability of Cp* relative to Cp. The CV of (η^5-Cp*)Co(Cab$^{S,S'}$)(CN^{t}Bu) (**2a**) has two major redox responses, that is, an irreversible 0/−1 wave ($E_{pc} = -1.66$ V) and a reversible 0/+1 wave ($E_{1/2} = 0.55$ V). Another small oxidation peak at −1.08 V is apparently due to the oxidation of the 16-electon complex **1**, which is produced by elimination of the Lewis base. The CV pattern is similar to that of (η^5-Cp)Co(Cab$^{S,S'}$)(CN^{t}Bu) except for an enhancement of the 0/+1 reversibility and a lack of other small peaks [3]. Both the reduction and oxidation potentials of **2a** shift towards the negative direction compared with those of **1**

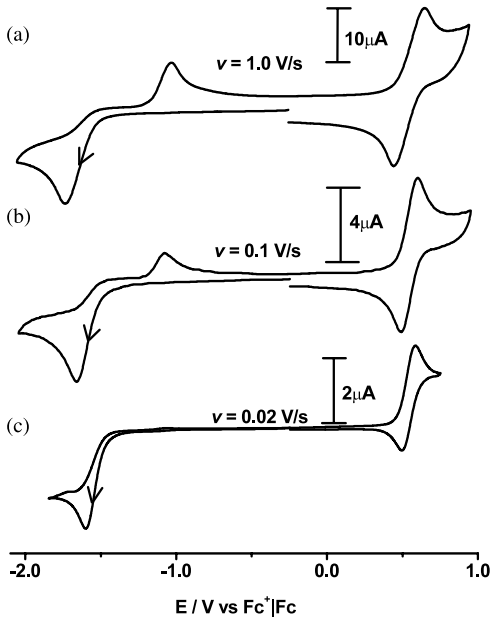

Fig. 3. Effect of the scan rate (v) on the CVs of (η^5-Cp*)Co(Cab$^{S,S'}$)(CN^{t}Bu) (**2a**); v = 1.0 (A); 0.10 (B); 0.020 V s^{-1} (C). Other conditions are the same as in Fig. 1.

by 0.52 and 0.24 V, respectively; this implies that both the metal and sulfur atoms become more electron rich by the addition of Lewis base.

The CVs of **2a** as a function of v are illustrated in Fig. 3. At $v = 1.0$ Vs^{-1}, the ratio of the anodic peak current (i_{pa}) at $E \approx -1.08$ V to the cathodic peak current (i_{pc}) at $E \approx -1.66$ V is 0.48. The same current ratio becomes smaller as the scan rate decreases, that is, 0.25 at $v =$ 0.10 V s^{-1} and virtually zero at $v = 0.020$ V s^{-1}. The oxidation peak at $E \approx -1.08$ V is not observed in the CV with a potential scan range between -0.15 and -1.35 V; however, it does appear in the CV of the first cycle with a potential scan range between -0.15 and -1.85 V but with only a vague hint of the corresponding re-reduction peak at the next cycle even with $v = 1.0$ V s^{-1} (data not shown). Thus, this behavior can be explained as follows: the CN^{t}Bu ligand is eliminated upon reduction of the electronically stable 18-electron complex **2a** due to the excess electron density, but the ligand remains near the coordination sphere to re-coordinate and therefore regenerate **2a** (Eq. (1); see more detailed mechanism is expected as in Refs. [7,8]). Judging from the potential scan rate, the re-coordination process is completed within a few seconds.

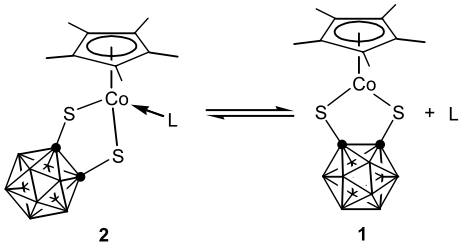

2 1 (1)

The CV of complex **2b** resembles that of **2a**, that is, it has an irreversible $0/-1$ wave ($E_{pc} = -1.65$ V), a reversible $0/+1$ wave ($E_{1/2} = 0.62$ V), and a small oxidation peak at -0.98 V. Both the reduction and oxidation potentials of **2b** are shifted towards the negative direction compared with those of **1** by 0.51 and 0.17 V, respectively. The CVs of **2b** as a function of v, which are also similar to the CVs given in Fig. 3 (not shown). However, the current ratios of i_{pa} at $E \approx -0.98$ V to i_{pc} at $E \approx -1.65$ V are 0.54 at $v = 1.0$ V s^{-1}, 0.33 at $v = 0.10$ V s^{-1}, and virtually zero at $v = 0.020$ V s^{-1}. Thus, a similar explanation for the CVs of **2a** can hold for **2b**, except that the current ratios for the reduction of the 18-electron complex indicate that a somewhat easier elimination of PMe_3 relative to CN^{t}Bu occurs.

The CV of **2c** displays rather complicated redox responses (two major reduction and two major oxidation waves), which were not observed with (η^5-Cp)Co(Cab$^{S,S'}$)(PEt_3) [3]. Two major reductions, that is, a reversible wave at $E_{1/2} = -1.08$ V and an irreversible one at $E_{pc} = -1.75$ V, and two major oxidations, that is, an irreversible wave near $E_{pa} = 0.52$ V and a quasi-reversible one at $E_{pa} = 0.85$ V, respectively, are

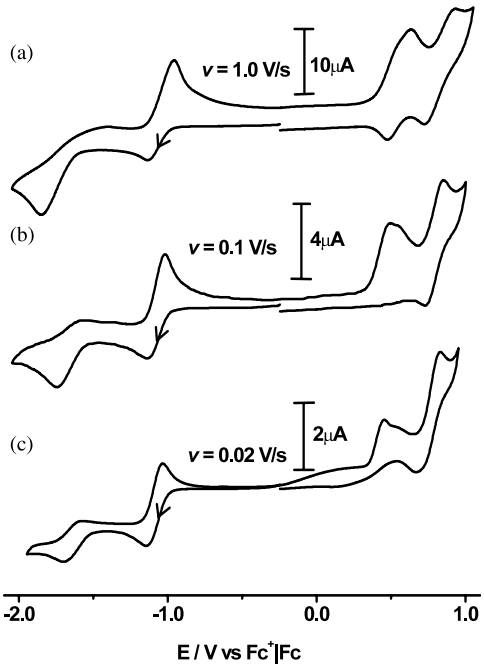

Fig. 4. Effect of the scan rate (v) on the CVs of (η^5-Cp*)Co(Cab$^{S,S'}$)(PEt_3) (**2c**); $v = 1.0$ (A); 0.10 (B); 0.020 V s^{-1} (C). Other conditions are the same as in Fig. 1.

observed. To understand the CV responses better, we also investigated the effect of v on the CV of **2c** (Fig. 4). By analyzing the CV obtained at $v = 1.0$ V s^{-1} (Fig. 4A), we can clearly separate it into the sum of two CVs: one is a CV with a reversible reduction and quasi-reversible oxidation wave near $E_{1/2} = -1.08$ and 0.79 V, respectively, which is the same as the CV of **1** (the 16-electon complex); the other is a CV with an irreversible reduction and quasi-reversible oxidation wave at $E_{pc} = -1.75$ and near 0.52 V, respectively. If we subtract the former CV from the CV in Fig. 4A, the resulting wave is expected to be a pure CV of the 18-electon complex **2c** free from other reactions. The shape of the resulting wave is also expected to be similar to that of **2a** or **2b**. Thus, we can say that both the $0/-1$ reduction and the $0/+1$ oxidation potentials of **2c** shift towards the negative direction compared with those of **1** by approximately 0.61 and 0.33 V, respectively, as in **2a** or **2b** but with larger amounts of shift.

Interestingly, the ratio of i_{pc} at $E \approx -1.14$ V to the i_{pc} at $E \approx -1.75$ V increases as v decreases. The ratios of the two i_{pc} values are 0.54, 1.1, and 2.0 at $v = 1.0$, 0.1, and 0.02 V s^{-1}, respectively. Thus, we suspect that the PEt_3 ligand is eliminated as the applied potential goes towards the negative direction and the ligand is too far from the coordination sphere to re-coordinate to the cobalt atom due to the enhanced steric interaction between the bulky Cp* and PEt_3 ligands. Such desorption of phosphine ligands is also reported for (η^5-Cp)Co($S_2C_2X_2$)(L) complexes previously [7,8].

The CV of **2d** (Fig. 2E) exhibits similar redox pattern as in **2c**. A reversible reduction wave at $E_{1/2} = -0.99$ V, an irreversible one at $E_{pc} = -1.52$ V, and two quasi-reversible oxidation waves near $E_{pa} = 0.71$ and 0.90 V, respectively, are observed. If we follow the earlier explanation, both the $0/-1$ reduction and the $0/+1$ oxidation potentials of **2d** shift towards the negative direction compared with those of **3** by approximately 0.37 and 0.14 V, respectively, as in **2a** or **2b** but with smaller amounts of shift. These small shifts of redox potentials imply that both the metal and sulfur atoms become less electron-rich on the addition of $PHPh_2$ than those of other ligands in **2a**–**c** due to the electron-withdrawing ability of the two phenyl moieties.

The CVs of **2d** as a function of v are also similar to Fig. 4 (not shown). Thus, the same explanation for the CVs of **2c** can be applied to the CVs of **2d**. The current ratios of i_{pc} at $E \approx -1.04$ V to i_{pc} at $E \approx -1.45$ V are 0.86, 2.2, and 3.5 at $v = 1.0$, 0.1 and 0.02 V s^{-1}, respectively. The cathodic current ratios imply that $PHPh_2$ is more easily eliminated than PEt_3 as the applied potential goes towards the negative direction. However, it is noteworthy that the first $0/+1$ oxidation wave (near $E_{pa} = 0.71$ V) is larger than the second $0/+1$ one (near $E_{pa} = 0.90$ V) (not shown), while both the $0/+1$ oxidation waves (near $E_{pa} = 0.52$ and 0.85 V) are almost the same in Fig. 4A. Judging from the relative size of the $0/+1$ oxidation waves, this behavior indicates that $PHPh_2$ is more difficult to eliminate than PEt_3 as the applied potential goes towards the positive direction.

Analyzing the CV results of **2** allows the following major conclusion to be drawn: the relatively large difference (0.19 V) between $E_{1/2}$ oxidation potentials (some are calibrated with $E_{1/2} = E_{pa} - (\Delta E_p, Fc^+/Fc)/2$) for **2b**–**d** suggests that the alkyl or aryl substituent on the phosphine moiety does influence the net electron donor ability of PR_3 to a significant extent; note that the substituent is far from the oxidation site (S atom) at three times the atom-to-atom distance (P atom to C atom of R group). The order of magnitude of the shifts of oxidation potentials of **2b**–**d** from **1** is $PHPh_2 < PMe_3 < PEt_3$, which parallels the basicity or the electronic effect of the PR_3 ligand. However, in fact our CV results imply that it becomes easier for **2** to eliminate/re-coordinate the L by oxidation to 1.0 V in the order $PMe_3 < PHPh_2$, PEt_3, in which the discrepant order of $PHPh_2$ and PMe_3 seems to be ascribed to a steric factor. Indeed, our observation agrees well with the increasing order of cone angle: PMe_3 (118°) < $PHPh_2$ (128°) < PEt_3 (132°) [9]. The failure of the synthesis of (η^5-Cp*)Co(Cab$^{S,S'}$)(PPh_3) also supports our argument. For example, in **2**, eight atoms are directly bonded to the metal. Inter-ligand repulsions are therefore common and relief of these repulsions on ligand dissociation favors ligand loss and makes the Co-P re-coordination more difficult. In particular, this effect may be even more pronounced for the bulky Cp* ancillary ligand than for Cp. However, it becomes easier for complex **2** to eliminate L by reduction in the order of $CN^tBu < PMe_3 < PEt_3 < PHPh_2$; here, electronic effects [10] are more pronounced than steric effects especially for PEt_3 and $PHPh_2$. The CV results of **2a**–**d** nicely illustrate the control of electrochemical behavior not only by the coordinating strength, but also by the cone angle of the ligands and the direction of redox. Again, such an effect was hard to be observed with the more spacious coordination complex of [(η^5-Cp)Co(Cab$^{S,S'}$)(L)]; the earlier report about the elimination/addition of the halides in [CpCoX(S_2C_2(COOMe)$_2$)(CHR$_2$)] [11a] is also compatible with our argument.

This part of our argument is also supported by the results shown in Fig. 5. The CV of (η^5-Cp*)Co(Cab$^{S,S'}$)($PHPh_2$) (**2d**) changes to that of (η^5-Cp*)Co(Cab$^{S,S'}$)(PMe_3) (**2b**) depending on the amount of PMe_3 added. In contrast, the CV of **2b** is independent of the amount of $PHPh_2$ added. However, no change of the peak positions was observed in the NMR spectra after mixing **2d** and PMe_3. These results convinced us that redox-induced ligand substitution reactions of (η^5-Cp*)Co(Cab$^{S,S'}$)(L) might be applied to an electrochemical *in situ* synthesis.

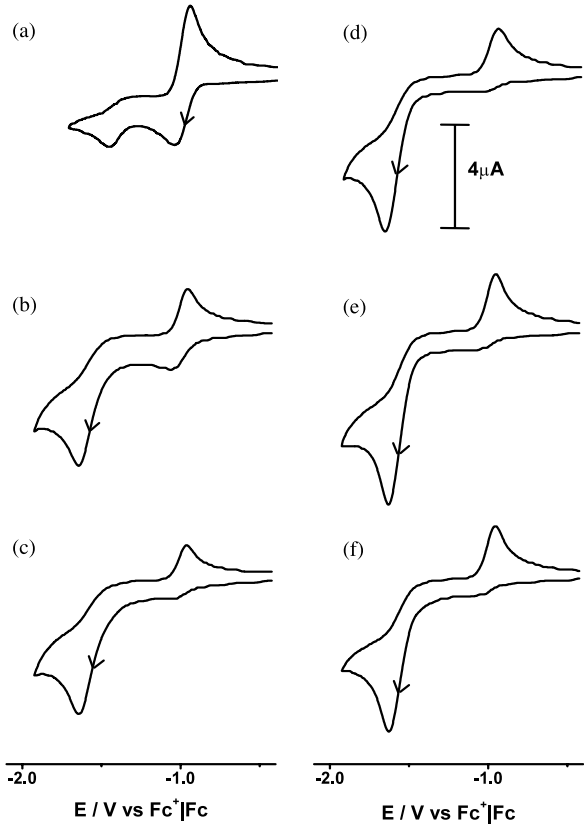

Fig. 5. The CVs of 1 mM (η^5-Cp*)Co(Cab$^{S,S'}$)($PHPh_2$) (**2d**) (A) in the presence of 0.4 mM (B) and 1 mM of PMe_3 (C), and 1 mM (η^5-Cp*)Co(Cab$^{S,S'}$)(PMe_3) (**2b**) (D) in the presence of 0.4 mM (E) and 1 mM of $PHPh_2$ (F). Other conditions are the same as in Fig. 1.

2.3. Addition reactions to the Co–S bonds of *1*

Recently, we reported alkylidene or acetylene addition reactions to the Co–S bonds of dithiolate **I** [4]. Consequently, we examined the electrochemical behavior of these alkylidene- or acetylene-bridged complexes and attempted to draw a comparison with their chemical behavior. The electrochemical results concerning the alkylidene- or acetylene-bridged complexes **3** are now described. Indeed, complex **1** was found to be a good precursor for such addition reactions as shown in Scheme 2 [11,12].

Treatment of **1** with the diazo compound $SiMe_3CHN_2$ afforded the soluble product [(η^5-Cp*)Co{η^3-(*S*,*S*′,*C*′)-$SC_2B_{10}H_{10}(CHSiMe_3)$}] (**3a**) in excellent yield (96%) after recrystallization (Scheme 2). Complex **3a** was isolated as an air-stable microcrystalline solid and was characterized by ^{1}H- and ^{13}C-NMR spectroscopy. Thus, the ^{1}H-NMR spectrum of complex **3a** had resonances for a trimethylsilyl group at δ 0.29 and a methine proton at δ 2.26. The ^{13}C-NMR spectrum had signals for the two types of carbons of the Cp* ring and the carbon atoms of the Co–S-substituted trimethylsilyl methine unit.

The CV of **3a** shows a well-defined reversible oxidation wave at $E_{1/2} = 0.19$ V, that is, the magnitude of potential shift is more than twice of that of **2** (Fig. 6B). The greater stability of the +1 oxidation state of **3a** compared to that of **2** seems to be ascribed to the coordination of the tridentate *S*,*S*,*C*-ligand as we reported for [(η^5-Cp)Co{η^3-(*S*,*S*′,*C*′)-$SC_2B_{10}H_{10}(CHSiMe_3)$}]. In contrast to the oxidation, the reduction responses of **3a** are more complicated and have three peaks, that is, a quasi-reversible reduction wave at $E_{1/2} = -1.06$ V and two irreversible ones near E_{pc} of -1.62 and -1.91 V. The first reduction wave near that of complex **1** becomes irreversible at the slower scan rate of 0.02 V s^{-1} (data not shown). In contrast to **3a**, a simple irreversible oxidation wave was observed for the analogous complex with Cp [3]. However, the electronic and steric effects of Cp* versus Cp allows us to speculate that Co–C coordination, or at least one coordination of the *S*,*S*,*C*-ligand, becomes loose as the applied potential goes towards the negative direction and the coordination is restored upon re-oxidation. A similar effect is also reported in the literature for the CVs of [(η^5-Cp)Co($S_2C_2(COOMe)_2$)(η^2-*C*,*C*-$CHSiMe_3$)] versus [(η^5-Cp)Co($S_2C_2(COOMe)_2$)(η^2-*C*,*C*–CPh_2)] [11c].

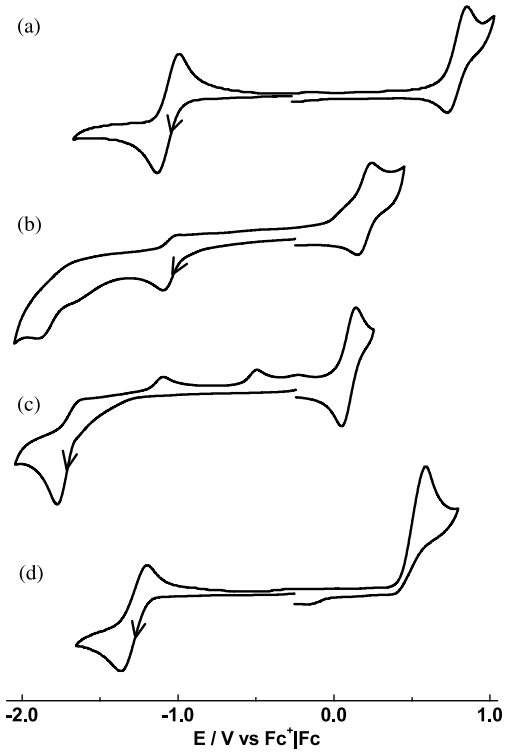

Fig. 6. The CVs of (η^5-Cp*)Co($Cab^{S,S'}$) (**1**) (A: for purpose of comparison) and [(η^5-Cp*)Co($Cab^{S,S'}$)(L)] [L = η^1-$CHSiMe_3$–*S* (**3a**) (B), η^1-HC=CPh–*S* (**3b**) (C), η^1-(COOMe)C=C(COOMe)–*S* (**3c**) (D)]. Other conditions are the same as in Fig. 1.

The cobaltadithia-*o*-carborane ring in **1** also undergoes addition to an acetylene unit between the Co and S atoms in its reaction with alkynes [1a–c,3,4,13]. Conversion of **1** to the corresponding metallabicyclic complexes **3b** and **3c** (Scheme 2) was expected to be favored by an electron-rich cobalt complex; therefore, we decided to investigate the reactivity of **1** towards a reactive phenyl acetylene and acetylenedicarboxylate. Treatment of **1** with one to two equivalents of the alkyne in refluxing toluene for 2 h indeed gave the alkyne adduct complexes, [(η^5-Cp*)Co{η^3-(*S*,*S*,*C*′)-$SC_2B_{10}H_{10}S(C'R_2)$}] [C′R_2 = HC=CPh (**3b**), (COOMe)C=

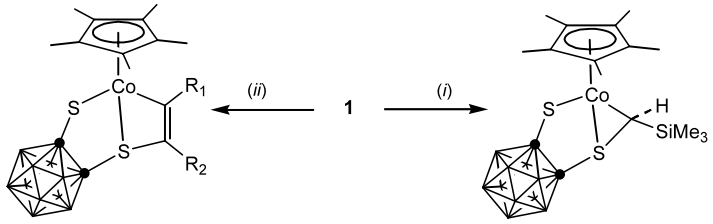

[(η^5-Cp*)Co($Cab^{S,S'}$)(η^1-R_1C=CR_2-S)] **3b-c**

(η^5-Cp*)Co($Cab^{S,S'}$)(μ-$CHSiMe_3$) **3a**

Scheme 2. Addition reaction of 16-electron metal complex **1** [a].

C(COOMe) (**3c**)], in moderate yield (Scheme 2). During the reaction, the color of the solution changed from red to orange yellow. Pure **3b** and **3c** were isolated in 35–89% yield after recrystallization. The complexes were characterized by a combination of elemental analysis and IR and NMR (^{1}H and ^{13}C) spectroscopy. The IR spectrum of **3b** has one C=C stretching band, and the ^{1}H-NMR spectrum of **3b** has the characteristic resonances of a coordinated olefin. Thus, the ^{1}H-NMR spectrum of **3b** shows the terminal proton at δ 2.36 and multiplet signals of the phenyl group of the acetylene at δ 7.53. Similarly, for **3c**, the OMe groups of the ester give rise to two singlets centered at δ 3.89 and 3.76, respectively. For the ^{13}C{^{1}H}-NMR spectra of **3c**, it is sufficient to point out that the resonances due to the π-bound olefin carbons are characteristically shifted upfield. The spectroscopic data of the cobalt complexes are in complete agreement with the proposed structure of **3c**.

The CV pattern of **3b** is similar to that of the 18-electron complex **2a** except for a difference in the potential of the 0/+1 oxidation wave at $E_{1/2} = 0.09$ V and a small irreversible re-oxidation peak at $E_{pa} = -0.50$ V (Fig. 6C). The two small irreversible oxidation peaks at $E_{pa} = -1.10$ and -0.50 V both disappear at the slower scan rate of 0.02 Vs^{-1} (data not shown). We also speculate that the Co–C bond of a coordinated olefin, and/or at least one coordination of the *S*,*S*,*C*-ligand, becomes loose as the applied potential goes towards the negative direction and leaves the S–C bond of a coordinated olefin intact. This may be indirect evidence that the reduction process takes place at the metal site.

Finally, the CV of **3c** has a quasi-reversible 0/−1 reduction wave at $E_{1/2} = -1.31$ V and an irreversible 0/+1 oxidation wave at $E_{pa} = 0.59$ V with a small reduction peak at $E_{pc} = -0.14$ V (Fig. 6D). The difference in oxidation potential between **3b** and **3c** is 0.46 V and the corresponding difference in reduction potential is 0.43 V; this indicates that the coordinated olefin in **3b** behaves as a stronger ligand than that in **3c** as was observed in (η^6-arene)Ru(Cab$^{S,S'}$)(L) complexes [4]. For the analogue with Cp, no clear redox features were observed [3], which might be ascribed to the redox instability. By changing the ligand from Cp to Cp*, we could obtain a well-defined CV; however, the CV pattern of **3c** does not belong to the general redox pattern of 18-electron complexes so far, that is, a reduced reversibility in both the reduction and oxidation waves was found. The irreversible oxidation peak seems to be somewhat larger than the reduction peak, which may suggest that the redox chemistry of **3c** involves some chemical reaction such as a self-electrocatalytic reaction. Overall, the changes of the redox properties of **3** with the ancillary ligands, Cp and Cp*, have been demonstrated clearly although we could not address them in detail.

3. Conclusion

We have examined the electrochemical behavior of the 16-electron species **1** and its 18-electron derivative **2**, in which some of the complexes exhibit elimination/re-coordination of Lewis bases. This may be applied to the in situ syntheses of new complexes through redox reactions starting from one of the aforementioned complexes. Moreover, we have demonstrated some possible CV patterns of 18-electron complexes depending on the nature of the complex. Thus, a rationale for the addition reaction with respect to the steric effects of the phosphine at the cobalt center based on the cone angle of the ligand has been established. The CV results of **2** may serve as a nice example to illustrate the control of electrochemical behavior not only by the coordinating strength, but also by the cone angle of the ligands and the direction of redox.

4. Experimental

4.1. General procedures

All manipulations were performed under a dry, oxygen-free, nitrogen or argon atmosphere using standard Schlenk techniques or in a Vacuum Atmosphere HE-493 dry box. THF was freshly distilled over potassium benzophenone. Toluene was dried and distilled from sodium benzophenone. Dichloromethane and hexane were dried and distilled over CaH_2. ^{13}C-, ^{1}H- and ^{31}P-NMR spectra were recorded on a Varian Mercury 300 spectrometer operating at 75.4, 300.0 and 121.4 MHz, respectively. All proton and carbon chemical shifts were measured relative to internal residual chloroform from the lock solvent (99.5% $CDCl_3$) and then referenced to Me_4Si (0.00 ppm). The ^{31}P-NMR spectra were recorded with 85% H_3PO_4 as an external standard. IR spectra were recorded on a Biorad FTS-165 spectrophotometer. Elemental analyses were performed with a Carlo Erba Instruments CHNS-O EA1108 analyzer. All melting points were uncorrected. All the electrochemical measurements were carried out in CH_2Cl_2 solutions containing 1 mM metal complex and 0.1 M tetrabutylammonium fluoroborate (TBAB), otherwise specified, at room temperature (r.t.) using a BAS 100B electrochemical analyzer. A platinum disk (dia. 1.6 mm) and platinum wire were used as a working and counter electrode. The reference electrode used was $Ag \mid AgNO_3$ and all the potential values shown were calibrated versus Fc/Fc^+ redox couple, unless otherwise specified. E_{pa} and E_{pc} denotes anodic and cathodic peak

potential, respectively, and $E_{1/2}$ value indicated is the average of E_{pa} and E_{pc} for the reversible redox waves.

o-Carborane was purchased from the Katechem and used without purification. Complex $Li_2Cab^{S,S'}$ [14] and $Cp^*Co(CO)I_2$ [15] were prepared according to the literature methods.

4.1.1. Preparation of $[(\eta^5\text{-}Cp^*)Co(Cab^{S,S'})]$ (1)

Representative procedure: a 3.2 mmol solution of $Li_2Cab^{S,S'}$ in THF (20 ml) was added to a stirred solution of $Cp^*Co(CO)I_2$ (1.43 g, 3.0 mmol) in THF (30 ml) cooled to -78 °C. The reaction mixture was then allowed to react at 0 °C for 1 h, and the solution was stirred for another 2 h at r.t. The solution gradually turned dark red, suggesting the formation of an *o*-carboranyl dithiolato metal complex. The solution was reduced in vacuo to about half its orginal volume, and some insoluble material was removed by filtration. The solution was removed under vacuum, and the resulting residue was taken up in a minimum of methylene chloride and then transferred to a column of silica gel. The crude residue was purified by column chromatography with hexane–$CHCl_3$ (90/10) affording >98% pure complex as red crystals. Red crystals of **1** were formed in 78% yield (0.94 g, 2.3 mmol). Data for **1**. Anal. Calc. for $C_{12}H_{25}B_{10}S_2Co$: C, 35.99; H, 6.29. Found: C, 36.63; H, 6.35%. IR (KBr, cm^{-1}): ν(B–H) 2590. ^{1}H-NMR (ppm, $CDCl_3$): 1.65 (s, 15H, *Cp**). $^{13}C\{^1H\}$-NMR (ppm, $CDCl_3$): 97.86 (s, *Cp**).

4.1.2. Reaction of 1 with CN^tBu

Under argon, CN^tBu (0.23 ml, 2.0 mmol) was added to a stirred solution of complex **1** (0.40 g, 1.0 mmol) in toluene (10 ml) cooled to 0 °C. The red solution immediately turned yellow. After stirring for 30 min, the solution was evaporated to dryness. The yellow residue of **2a** was dried in vacuo. Yield: 0.46 g (0.95 mmol, 95%). Data for **2a**. Anal. Calc. for $C_{17}H_{34}B_{10}S_2CoN$: C, 42.22; H, 7.09; N, 2.89. Found: C, 43.00; H, 7.11; N, 2.92%. IR (KBr, cm^{-1}): ν(C–H) 2985, 2915, ν(B–H) 2560, ν(C=N) 2181. ^{1}H-NMR (ppm, $CDCl_3$): 1.60 (s, 9H, N^tBu), 1.49 (s, 15H, *Cp**). $^{13}C\{^1H\}$-NMR (ppm, $CDCl_3$): 97.99 (s, *Cp**), 29.96 (s, CN^tBu), 9.96 (s, *Me* of Cp*), 8.43 (s, CN^tBu).

4.2. General synthesis of $[(\eta^5\text{-}Cp^*)Co(Cab^{S,S'})(L)]$ [L = PMe_3 (2b), PEt_3 (2c), $PHPh_2$ (2d)]

4.2.1. Reaction of 1 with PMe_3

Under argon, PMe_3 (2.0 mmol) was added to a red solution of complex **1** (0.40 g, 1.0 mmol) in 10 ml of methylene chloride. The resultant yellow solution was stirred for 30 min and evaporated to dryness. The yellow residue of **2b** was dried in vacuo. Yield: 0.40 g (0.85 mmol, 85%). Data for **2b**. Anal. Calc. for $C_{15}H_{34}B_{10}S_2CoP$: C, 37.80; H, 7.19. Found: C, 38.00; H, 7.25%. IR (KBr, cm^{-1}): ν(B–H) 2911, ν(B–H) 2557, 2585, ν(P–C) 1016. ^{1}H-NMR (ppm, $CDCl_3$): 1.50 (d, 9H, PMe_3, $^2J_{P-H} = 10.2$ Hz), 1.50 (d, 15H, *Cp** $J_{P-H} = 1.8$ Hz). $^{13}C\{^1H\}$-NMR (ppm, $CDCl_3$): 97.21 (s, *Cp**), 10.94 (d, $P(CH_3)_3$, $J_{P-C} = 44.59$ Hz), 9.11 (s, *Me* of Cp*),. $^{31}P\{^1H\}$-NMR (ppm, $CDCl_3$): 7.85 (s, PMe_3).

4.2.2. Analytical data for 2c

Complex **2c** was prepared from 0.40 g (1.0 mmol) of **1**. After recrystallization with hexane–CH_2Cl_2 (90/10), **2c** (82%) was isolated as a yellow solid. Data for **2c**. Anal. Calc. for $C_{18}H_{40}B_{10}S_2CoP$: C, 41.68; H, 7.77. Found: C, 41.80; H, 7.82%. IR (KBr, cm^{-1}): ν(C–H) 2970, 2907, 2878, ν(B–H) 2576, 2559, ν(P–C) 1032. ^{1}H-NMR (ppm, $CDCl_3$): 1.97 (dq, 6H, PCH_2, $^3J_{P-H} = 9.2$ Hz, $^1J_{H-H} = 7.5$ Hz), 1.47 (s, 15H, *Cp**), 1.03 (dt, 9H, PCH_2Me, $^3J_{P-H} = 14.4$ Hz, $^1J_{H-H} = 7.7$ Hz). $^{13}C\{^1H\}$-NMR (ppm, $CDCl_3$): 96.72 (s, *Cp**), 30.22 (s, $P(CH_2Me)_3$), 17.65 (d, $^1J_{P-C} = 26$ Hz, $P(CH_2Me)_3$), 9.86 (s, *Me* of Cp*). $^{31}P\{^1H\}$-NMR (ppm, $CDCl_3$): 20.43 (s, PEt_3).

4.2.3. Analytical data for 2d

Complex **2d** was prepared from 0.40 g (1.0 mmol) of **1**. After recrystallization with hexane/toluene (90/10), **2d** (94%) was isolated as a yellow solid. Data for **2d**. Anal. Calc. for $C_{24}H_{36}B_{10}S_2CoP$: C, 49.13; H, 6.18. Found: C, 49.55; H, 6.23%. IR (KBr, cm^{-1}): ν(C–H) 2905, ν(B–H) 2560, ν(P–C) 1096. ^{1}H-NMR (ppm, $CDCl_3$): 7.66 (m, PC_6H_5), 7.47 (m, PC_6H_5), 7.32 (m, PC_6H_5), 2.5 (br, 1H, $PHPh_2$), 1.34 (s, 15H, *Cp**). $^{13}C\{^1H\}$-NMR (ppm, $CDCl_3$): 133.85, 129.18, 128.74, 128.37 ($HPPh_2$), 97.09 (s, *Cp**), 9.91 (s, *Me* of Cp*). ^{31}P-NMR (ppm, $CDCl_3$): 21.67 (d, $^1J_{P-H} = 432.7$ Hz, $PHPh_2$).

4.2.4. Reaction of 1 with Me_3SiCHN_2

A solution of complex **1** (0.40 g, 1.0 mmol) in toluene (20 ml) was treated with a 2.0 M hexane solution of (trimethylsilyl)diazomethane (0.6 ml, 1.2 mmol) at r.t. for 5 min. The red color of the solution quickly faded to give a yellow solution. The volatile substances were then removed in vacuo, and the resulting solid was extracted with CH_2Cl_2. Addition of hexane to the concentrated extract gave complex **3a** as yellow–orange crystals. Yield: 0.47 g (0.96 mmol, 96%). Data for **3a**. Anal. Calc. for $C_{16}H_{35}B_{10}S_2CoSi$: C, 39.48; H, 7.25. Found: C, 39.66; H, 7.32%. IR (KBr, cm^{-1}): ν(C–H) 2955, 2910, ν(B–H) 2586. ^{1}H-NMR (ppm, $CDCl_3$): 2.26 (s, 1H, Me_3SiCH), 1.65 (s, 15H, *Cp**), 0.29 (s, 9H, $SiMe_3$). $^{13}C\{^1H\}$-NMR (ppm, $CDCl_3$): 92.93 (s, *Cp**), 39.24 (s, Me_3SiCH), 10.59 (s, *Me* of Cp*), 1.43 (s, $SiMe_3$), 1.17 (s, $SiMe_3$).

4.3. General synthesis of [(η^5-Cp*)Co{η^3-(S,S,C′)-$SC_2B_{10}H_{10}S(C'R_2)$}] [$C'R_2$ = HC=CPh (**3b**), (COOMe)C=C(COOMe) (**3c**)]

In a typical run **1** (1.0 mmol) and alkynes were dissolved in toluene (15 ml) under argon and the solution was stirred for 8 h at r.t. The red color of the solution slowly faded to give a yellow solution, suggesting the formation of an adduct. The completion of the reaction was monitored by TLC. The solution was reduced in vacuo to about half its original volume, and some insoluble material was removed by filtration. Addition of hexane to the resulting solution afforded **3b**–**c** as a dark yellow precipitate.

4.3.1. Analytical data for **3b**

Complex **3b** was prepared from 2.0 mmol (0.22 ml) of phenylacetylene. After recrystallization from toluene, **3b** (0.18 g, 0.35 mmol, 35% yield) was isolated as a yellow solid. Anal. Calc. for $C_{20}H_{31}B_{10}S_2Co$: C, 47.79; H, 6.22. Found: C, 47.84; H, 6.30%. IR (KBr, cm^{-1}): ν(B–H) 2591, ν(C=C) 1590, ν(C=C) 1486. ^{1}H-NMR (ppm, $CDCl_3$): 7.53 (m, 5H, *Ph*), 2.36 (s, 1H, C=C*H*), 1.24 (s, 15H, *Cp**). $^{13}C\{^1H\}$-NMR (ppm, $CDCl_3$): 193.07 (s, HC=CPh), 176.66 (s, HC=CPh), 130.10 (m, *Ph*), 93.36 (s, *Cp**), 9.92 (*Me* of Cp*).

4.3.2. Analytical data for **3c**

Complex **3c** was prepared from 2.0 mmol (0.25 ml) of dimethyl acetylenedicarboxylate. After recrystallization from toluene, **3c** (0.48 g, 0.89 mmol, 89% yield) was isolated as a yellow solid. Anal. Calc. for $C_{18}H_{31}B_{10}S_2CoO_4$: C, 39.84; H, 5.76. Found: C, 40.02; H, 5.82%. IR (KBr, cm^{-1}): ν(C–H) 2951, 2908, 2847, ν(B–H) 2584, ν(CO) 1710, ν(C=C) 1573. ^{1}H-NMR (ppm, $CDCl_3$): 3.89 (s, 3H, O*Me*), 3.76 (s, 3H, O*Me*), 1.48 (s, 15H, *Cp**). $^{13}C\{^1H\}$-NMR (ppm, $CDCl_3$): 185.74 (s, MeO*C*O), 119.78 (s, MeOCO*C*=), 98.91 (s, *Cp**), 95.48 (s, *Cp**), 78.82 (s, O*Me*), 9.43 (*Me* of Cp*), 9.34 (*Me* of Cp*).

4.4. X-ray crystallography

Suitable crystals of **2d** were obtained by slow diffusion of hexane into a toluene solution of the complexes at r.t. and were mounted on a glass fiber. Crystal data and experimental details are given in Table 2. The data set for **2d** were collected on an Enraf CAD4 automated diffractometer. Mo–K_α radiation (λ = 0.7107 Å) was used for all structures. Each structure was solved by the application of direct methods using the SHELXS-96 program [16a] and least-squares refinement using SHELXL-97 [16b]. All non-hydrogen atoms in compound **2d** were refined anisotropically. All other hydrogen atoms were included in calculated positions (Table 3).

Table 2
Crystal data and structure refinement for **2d**·C_7H_8

Identification code	kor291
Empirical formula	$C_{31}H_{44}B_{10}PS_2Co$
Formula weight	678.84
Temperature (K)	293(2)
Wavelength (Å)	0.71070
Crystal system	Orthorhombic
Space group	*Pbca*
Unit cell dimensions	
a (Å)	15.863(1)
b (Å)	20.534(1)
c (Å)	21.868(2)
V (Å^3)	7123.1(8)
Z	8
D_{calc} (g cm^{-3})	1.266
μ (mm^{-1})	0.666
F(000)	2768
Crystal size (mm^3)	0.3 × 0.45 × 0.45
θ Range for data collection (°)	1.86–25.97
Index ranges	$0 \le h \le 19$, $0 \le k \le 25$, $0 \le l \le 27$
Reflections collected/unique	6981/6981 [R_{int} = 0.0000]
Refinement method	Full-matrix least-squares on F^2
Data/restraints/parameters	6978/0/400
Goodness-of-fit on F^2	1.039
Final *R* indices [I > 2σ(I)]	R_1 [a] = 0.0653, wR_2 [b] = 0.1603
R indices (all data)	R_1 [a] = 0.1713, wR_2 [b] = 0.2117
Largest difference peak and hole (e·Å^{-3})	0.676 and −0.339

[a] $R_1 = \Sigma||F_o| - |F_c||$ (based on reflections with $F_o^2 > 2\sigma F^2$).
[b] $wR_2 = [\Sigma[w(F_o^2 - F_c^2)^2]/\Sigma[w(F_o^2)^2]]^{1/2}$; $w = 1/[\sigma^2(F_o^2) + (0.095P)^2]$; $P = [\max(F_o^2, 0) + 2F_c^2]/3$ (also with $F_o^2 > 2\sigma F^2$).

Table 3
Selected bond lengths (Å) and bond angles (°) in **2d**·C_7H_8

Bond lengths			
Co(1)–S(1)	2.253(2)	Co(1)–S(2)	2.258(2)
Co(1)–P(1)	2.204(2)	S(1)–C(1)	1.791(6)
S(2)–C(2)	1.777(6)	P(1)–C(13)	1.830(6)
P(1)–C(19)	1.833(7)	C(1)–C(2)	1.666(8)
Bond angles			
P(1)–Co(1)–S(1)	87.56(6)	P(1)–Co(1)–S(2)	87.24(7)
S(1)–Co(1)–S(2)	93.23(6)	C(1)–S(1)–Co(1)	104.9(2)
C(2)–S(2)–Co(1)	105.1(2)	C(13)–P(1)–C(19)	103.4(3)
C(13)–P(1)–Co(1)	121.5(2)	C(19)–P(1)–Co(1)	117.9(2)

5. Supplementary material

Crystallographic data for the structural analysis have been deposited with the Cambridge Crystallographic Data Centre, CCDC no. 214276 for compound **2d**. Copies of this information may be obtained free of charge from The Director, CCDC, 12 Union Road, Cambridge CB2 1EZ, UK (Fax: +44-1223-336033; e-mail: deposit@ccdc.cam.ac.uk or www: http://www.ccdc.cam.ac.uk).

Acknowledgements

We thank Prof. Sukbok Chang at the Korean Advanced Institute of Science and Technology (KAIST) for helpful discussions. Financial support from the Korean Science & Engineering Foundation (R01-2000-00050) and the Korea Research Foundation (2001-041-D00119) is gratefully acknowledged.

References

[1] (a) J. Ko, S.O. Kang, Adv. Organomet. Chem. 47 (2001) 61;
(b) J.-Y. Bae, Y.-J. Lee, S.-J. Kim, J. Ko, S. Cho, S.O. Kang, Organometallics 19 (2000) 1514;
(c) D.-H. Kim, J. Ko, K. Park, S. Cho, S.O. Kang, Organometallics 18 (1999) 2738;
(d) J.-Y. Bae, Y.-I. Park, J. Ko, K.-I. Park, S.-I. Cho, S.O. Kang, Inorg. Chim. Acta 289 (1999) 141.

[2] (a) K. Base, M.W. Grinstaff, Inorg. Chem. 37 (1998) 1432;
(b) O. Crespo, M.C. Gimeno, P.G. Jones, A. Laguna, J. Chem. Soc. Dalton Trans. (1997) 1099;
(c) O. Crespo, M.C. Gimeno, P.G. Jones, A. Laguna, J. Chem. Soc. Chem. Commun. (1993) 1696;
(d) J.G. Contreras, L.M. Silva-trivino, M.E. Solis, J. Coord. Chem. 14 (1986) 309;
(e) H.D. Smith, Jr, M.A. Robinson, S. Papetti, Inorg. Chem. 6 (1967) 1014;
(f) H.D. Smith, Jr, C.O. Obenland, S. Papetti, Inorg. Chem. 5 (1966) 1013;
(g) H.D. Smith, Jr, J. Am. Chem. Soc. 87 (1965) 1817.

[3] J.-H. Won, D.-H. Kim, B.Y. Kim, S.-J. Kim, C. Lee, S. Cho, J. Ko, S.O. Kang, Organometallics 21 (2002) 1443.

[4] J.-H. Won, H.-G. Lim, B.Y. Kim, J.-D. Lee, C. Lee, Y.-J. Lee, S. Cho, J. Ko, S.O. Kang, Organometallics 21 (2002) 5703.

[5] M. Herberhold, H. Yan, W. Milius, J. Organomet. Chem. 598 (2000) 142.

[6] (a) R.I. Michelman, G.E. Ball, R.G. Bergmen, R.A. Anderson, Organometallics 13 (1994) 869;
(b) J.J. Garcia, H. Torrens, H. Adames, N.A. Bailey, A. Scacklady, P.M. Matlis, J. Chem. Soc. Dalton Trans. (1993) 1529;
(c) R.I. Michelman, R.A. Anderson, R.G. Bergman, J. Am. Chem. Soc. 113 (1991) 5100;
(d) J.J. Garcia, H. Torrens, H. Adams, N.A. Bailey, P.M. Maitlis, J. Chem. Soc. Chem. Commun. (1991) 74;
(e) D.P. Klein, G.M. Kloster, R.G. Bergman, J. Am. Chem. Soc. 112 (1990) 2022.

[7] K. Shimizu, H. Ikehara, M. Kajitani, H. Ushijima, T. Akiyama, A. Sugimori, G.P. Satô, J. Electroanal. Chem. 396 (1995) 465.

[8] A. Sugimori, T. Akiyama, M. Kajitani, T. Sugiyama, Bull. Chem. Soc. Jpn. 72 (1999) 879.

[9] (a) P.W.N.M. van Leeuwen, P.C.J. Kamer, J.N.H. Reek, P. Dierkes, Chem. Rev. 100 (2000) 2741;
(b) C.A. Tolman, Chem. Rev. 77 (1977) 313.

[10] (a) M.N. Golovin, M.M. Rahman, J.E. Belmonte, W.P. Giering, Organometallics 4 (1985) 1981;
(b) C.A. Tolman, J. Am. Chem. Soc. 92 (1970) 2953.

[11] (a) C. Takayama, K. Takeuchi, S. Ohokoshi, M. Kajitani, T. Sugiyama, A. Sugimori, Organometallics 18 (1999) 4032;
(b) C. Takayama, K. Takeuchi, S. Ohokoshi, G.C. Janairo, T. Sugiyama, M. Kajitani, A. Sugimori, Organometallics 18 (1999) 2843;
(c) C. Takayama, M. Kajitani, T. Sugiyama, A. Sugimori, J. Organomet. Chem. 563 (1998) 161;
(d) C. Takayama, K. Takeuchi, M. Kajitani, T. Sugiyama, A. Sugimori, Chem. Lett. (1998) 241;
(e) M. Sakurada, M. Kajitani, K. Dohki, T. Akiyama, A. Sugimori, J. Organomet. Chem. 423 (1992) 141;
(f) M. Sakurada, J. Okubo, M. Kajitani, T. Akiyama, A. Sugimori, Phosphorus, Sulfur, Silicon, Relat. Elements 67 (1992) 145;
(g) M. Kajitani, M. Sakurada, K. Dohki, T. Suetsugu, T. Akiyama, A. Sugimori, J. Chem. Soc. Chem. Commun. (1990) 19;
(h) M. Sakurada, J. Okubo, M. Kajitani, T. Akiyama, A. Sugimori, Chem. Lett. (1990) 1837.

[12] (a) M. Kajitani, T. Suetsugu, T. Takagi, T. Akiyama, A. Sugimori, K.H. Yamazaki, J. Organomet. Chem. 487 (1995) C8;
(b) M. Sakurada, M. Kajitani, K. Dohki, T. Akiyama, A. Sugimori, J. Organomet. Chem. 423 (1992) 141;
(c) M. Kajitani, T. Suetsugu, R. Wakabayashi, A. Igarashi, T. Akiyama, A. Sugimori, J. Organomet. Chem. 293 (1985) C15.

[13] (a) M. Herberhold, H. Yan, W. Milius, B. Wrackmeyer, J. Chem. Soc. Dalton Trans. (2001) 1782;
(b) M. Herberhold, H. Yan, W. Milius, B. Wrackmeyer, J. Organomet. Chem. 623 (2001) 149;
(c) M. Herberhold, H. Yan, W. Milius, B. Wrackmeyer, Organometallics 19 (2000) 4289;
(d) M. Herberhold, H. Yan, W. Milius, B. Wrackmeyer, J. Organomet. Chem. 604 (2000) 170;
(e) M. Herberhold, H. Yan, W. Milius, B. Wrackmeyer, Chem. Eur. J. 6 (2000) 3026;
(f) M. Herberhold, H. Yan, W. Milius, B. Wrackmeyer, Z. Anorg. Allg. Chem. 626 (2000) 1627;
(g) M. Herberhold, H. Yan, W. Milius, B. Wrackmeyer, Angew. Chem. Int. Ed. Engl. 38 (1999) 3689;
(h) M. Herberhold, G.-X. Jin, H. Yan, W. Milius, B. Wrackmeyer, Eur. J. Inorg. Chem. (1999) 873;
(i) M. Herberhold, G.-X. Jin, H. Yan, W. Milius, B. Wrackmeyer, J. Organomet. Chem. 587 (1999) 252.

[14] H.D. Smith, Jr, C.O. Obenland, S. Papetti, Inorg. Chem. 5 (1966) 1013.

[15] S.A. Frith, J.L. Spencer, Inorg. Synth. 28 (1990) 273.

[16] (a) G.M. Sheldrick, Acta. Crystallogr. Sect. A 46 (1990) 467;
(b) G.M. Sheldrick, SHELXL-97, Program for Crystal Structure Refinement, University of Göttinen, Germany, 1997.